High-resolution Mapping of Forest Carbon Stocks in the Colombian Amazon

Supplementary Material

(I) Field validation

A summary of the allometric equations used, and species encountered is provided in Tables S1 and S2, respectively.

(II) Model fitting techniques

The ACD validation model (eq. 3) and H-D model (Table S1) were each fit using non-linear Maximum Likelihood Analysis in R, and by incorporating a third equation parameter in the form of a non-arithmetic error term (i.e., $y = ax^b + x^k * \varepsilon$) to account for heteroscedasticity common to previously published ACD-MCH and H-D relationships. This fitting technique is analogous to fitting a linear model to log-transformed x and y data, thereby avoiding the need for log-transformation and back-transformation (Baskerville, 1972; Mascaro et al., 2011b).

(III) Additional information about the regional stratification approach

For the final regional stratification, a total of 147 Landsat Thematic Mapper (TM) and Enhanced Thematic Mapper Plus (ETM+) images were processed through CLASlite. This dataset included 72 images for 2010, 31 for 1990, 20 for 2000, and 24 for 2005. Employing a semi-automated approach to masking clouds, smoke, haze and shadows, we constructed cloud-free regional maps at 30 m resolution.

Median ACD values determined from LiDAR-scale ACD for each land-cover class are listed in Table S3. If a class in the final stratification map did not contain sufficient LiDAR coverage (e.g., less than the targeted 1% or less than 100 ha), we assigned the median ACD value of a broader class on the preceding node of the stratification decision tree (Figure 2c of main text). For example, if the high TRI stratum for a particular catchment did not have sufficient coverage, we assigned the median ACD value of the same TRI stratum for all catchments.

For the stratification approach, catchment boundaries were derived from SRTM data (Hydrology Toolbox, ArcGIS 10, ESRI Inc., USA), which resulted in additional ACD sub-stratification by more than 60 Mg C ha^{-1} in some cases. This addition – supported by a stratification approach – allowed for capturing discrete geographic changes in carbon stocks that may otherwise have been missed in the regional analyses, similar to the localized effects of terrain variation as expressed in the TRI.

(IV) Regression equation used for continuous fields map of ACD

Following the results of the correlation analyses (see Methods of main text), we conducted multiple least squares regression analyses using elevation (ELEV), slope, aspect and a terrain ruggedness index (TRI) derived from NASA Shuttle Radar Topography Mission (SRTM) data, and photosynthetic vegetation coverage fraction (PV) and soil cover fraction derived from CLASlite. Through iterations of regression analyses using all of these variables, as well as their interaction terms, we determined that only PV and ELEV influenced the fit of the model at the scale of the entire study region. The final least squares regression of these variables yielded the following model:

$$ACD = -3553.5097 - 0.1691 \times ELEV + 79.9664 \times PV - 0.4323 \times PV^2$$

with an adjusted r^2 of 0.20 and a residual standard error of 33.85 Mg C ha^{-1}. All terms were significant at $P < 0.0001$. This equation, which ingested all available LiDAR data was used estimate ACD at the regional level.

While the above model was used for final mapping (i.e., in conjunction with non-forest carbon stock estimations from CLASlite), we also created a second model using a 75% subset of the LiDAR data for the purposes of estimating errors in the remaining 25% of the data. This model was:

$$ACD = -3669.4719 - 0.1672 \times ELEV + 82.5010 \times PV - 0.4462 \times PV^2$$

with an adjusted r^2 of 0.19 and a residual standard error of 34.19 Mg C ha^{-1}. All terms were significant at $P < 0.0001$.

(V) Sources of error in linking LiDAR-based and plot-based estimates of ACD

Standard plot protocol in the field (e.g., Condit, 1998) dictates that trees are considered to be inside a plot if more than 50% of their main stem is contained within the plot boundary. However, LiDAR energy is returned by the 3-D components of forest canopies, including tree crowns and branches. Thus, a plot within the LiDAR coverage includes portions of crowns that overhang the edge of the plot, and excludes portions that extent beyond the plot edge. In effect, this disagreement between LiDAR and field estimated ACD produces a false error in typical LiDAR calibrations, including those of the type underlying the universal LiDAR model. Plot size also has a considerable effect, with errors decreasing as plot size increases according to the inverse square root of the plot area.

Mascaro et al. (2011a) demonstrated the propagation of each of these errors using a 50-ha plot with mapped trees. Empirically, relative errors were 23 Mg C ha^{-1} at 0.09 ha resolution (i.e., a median value based on measurements at 0.08 and 0.1 ha resolution), or 21.5% of the mean

carbon stock of the entire 50-ha area (107 Mg C ha^{-1}). Likewise, errors were 10.7 Mg C ha^{-1} at 1 ha resolution (10.0%).

Supplemental References

Asner, G. P., Powell, G. V. N., Mascaro, J., Knapp, D. E., Clark, J. K., Jacobson, J., Kennedy-Bowdoin, T., Balaji, A., Paez-Acosta, G., Victoria, E., Secada, L., Valqui, M., and Hughes, R.F.: High-resolution forest carbon stocks and emissions in the Amazon, P. Natl. A. Sci., 107, 16738-16742, 2010.

Baskerville, G.: Use of logarithmic regression in the estimation of plant biomass, Canadian Journal of Forest Research-Revue Canadienne De Recherche Forestiere, 2, 49-53, 1972.

Chao, K.-J., Phillips, O. L., Baker, T. R., Peacock, J., Lopez-Gonzalez, G., Vásquez Martínez, R., Monteagudo, A., and Torres-Lezama, A.: After trees die: Quantities and determinants of necromass across amazonia, Biogeosciences, 6, 1615-1626, 2009.

Chave, J., Andalo, C., Brown, S., Cairns, M. A., Chambers, J. Q., Eamus, D., Fölster, H., Fromard, F., Higuchi, N., Puig, H., Riéra, B., and Yamakura, T.: Tree allometry and improved estimation of carbon stocks and balance in tropical forests, Oecologia, 145, 87-99, DOI 10.1007/s00442-005-0100-x, 2005.

Chave, J., Coomes, D., Jansen, S., Lewis, S. L., Swenson, N. G., and Zanne, A. E.: Towards a worldwide wood economics spectrum, Ecology Letters, 12, 351-366, 2009.

Condit, R.: Tropical forest census plots, Springer-Verlag and R. G. Landes Company, Berlin, Germany and Georgetown, Texas, USA, 1998.

Mascaro, J., Detto, M., Asner, G. P., and Muller-Landau, H. C.: Evaluating uncertainty in mapping forest carbon with airborne LiDAR, Remote Sens. Environ., 115, 3770-3774, 2011a.

Mascaro, J., Litton, C. M., Hughes, F. R., Uowolo, A., and Schnitzer, S. A.: Minimizing bias in biomass allometry: Model selection and log-transformation of data, Biotropica, 43, 649-653, 2011b.

Riley, S. J., DeGloria, S. D., and Elliot, R.: A terrain ruggedness index that quantifies topographic heterogeneity, Intermountain Journal of Science, 5, 23-27, 1999.

ter Steege, H., Pitman, N. C. A., Phillips, O. L., Chave, J., Sabatier, D., Duque, A., Molino, J. F., Prevost, M. F., Spichiger, R., Castellanos, H., von Hildebrand, P., and Vasquez, R.: Continental-scale patterns of canopy tree composition and function across amazonia, Nature, 443, 444-447, 10.1038/nature05134, 2006.

Supplemental Figures

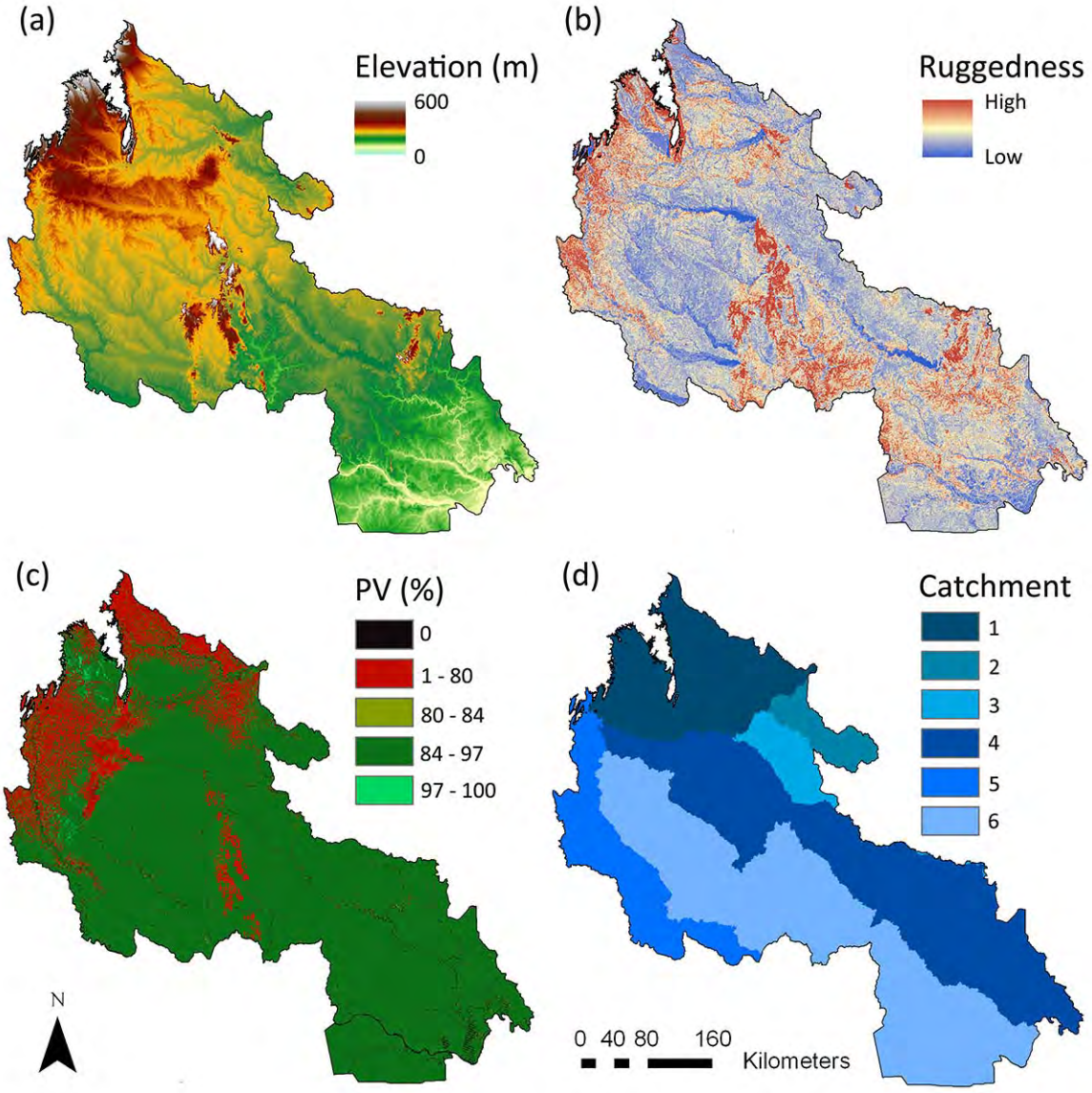

Figure S1. Selected variables used to stratify the study area: (a) digital elevation model (DEM) derived from the NASA Shuttle Radar Topography Mission (STRM), (b) terrain ruggedness index (TRI), (c) fractional cover of photosynthetic vegetation (PV) derived from CLASlite, and (d) drainage catchments. Elevation and PV were also used as inputs to the regression approach.

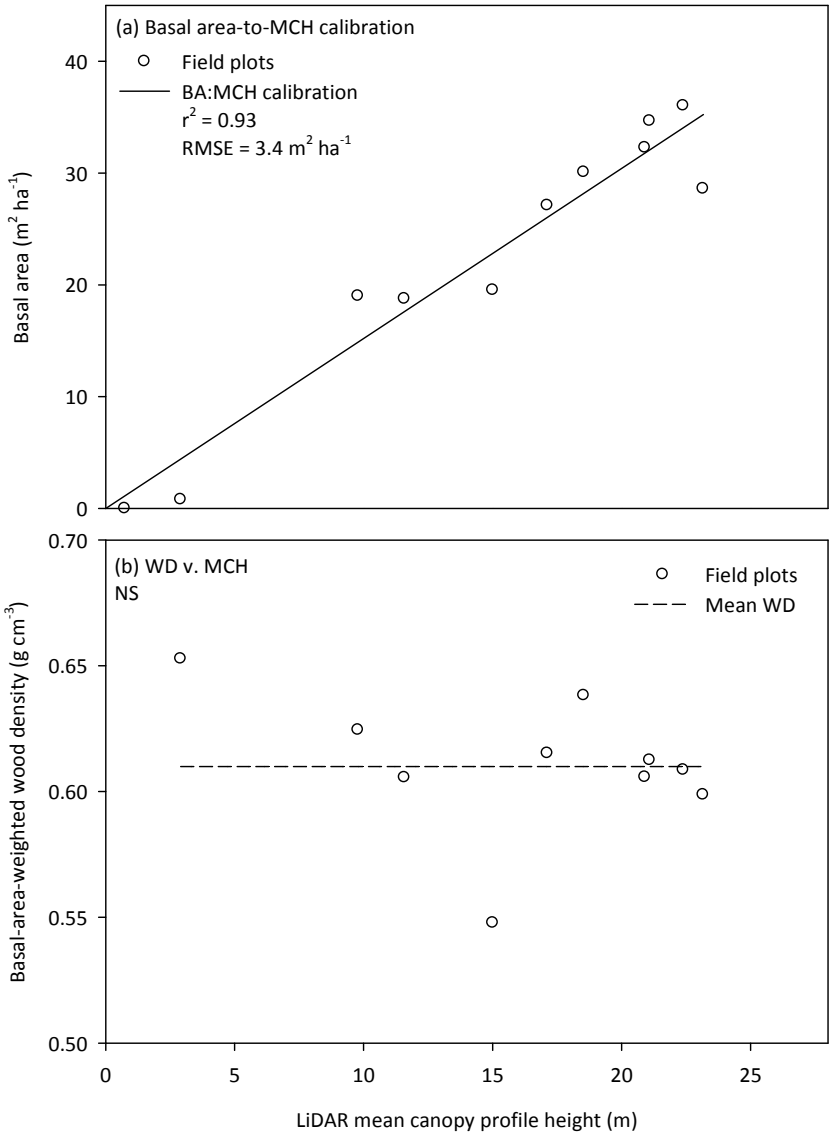

Figure S2. (a) Relationship between field-estimated basal area and LiDAR-derived mean canopy profile height (termed the Stocking Coefficient). (b) Relationship between basal-area-weighted wood density and LiDAR derived mean canopy profile height.

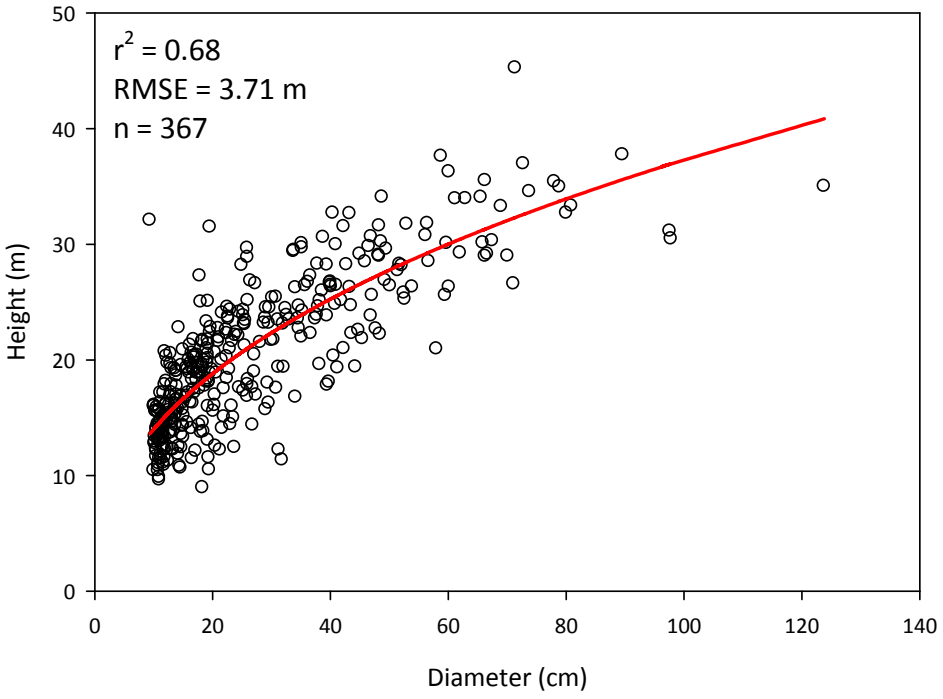

Figure S3. Height to diameter relationship among 367 trees measured in the field plots. All trees > 50 cm dbh were measured for height, as well as several trees of smaller diameters. For field ACD validation, heights of the remaining smaller trees were estimated using the model as shown (model parameters in Table S1).

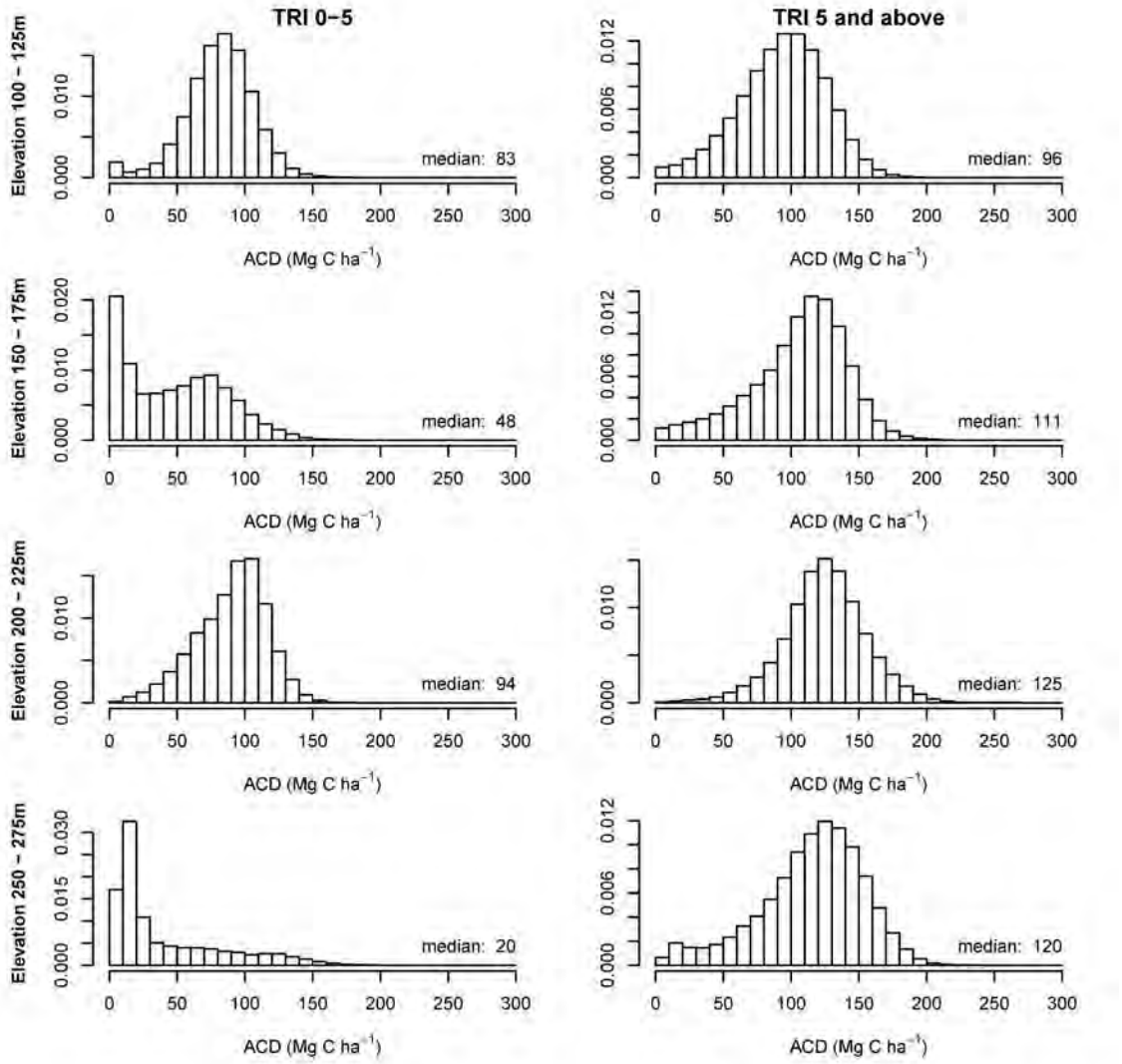

Figure S4. Differences in the distribution of forest aboveground carbon density (ACD) at different elevations for landscapes with low (0-5) and high (5+) values of the terrain ruggedness index (TRI; Riley et al., 1999). Median ACD values for each distribution are shown in the lower right of each panel.

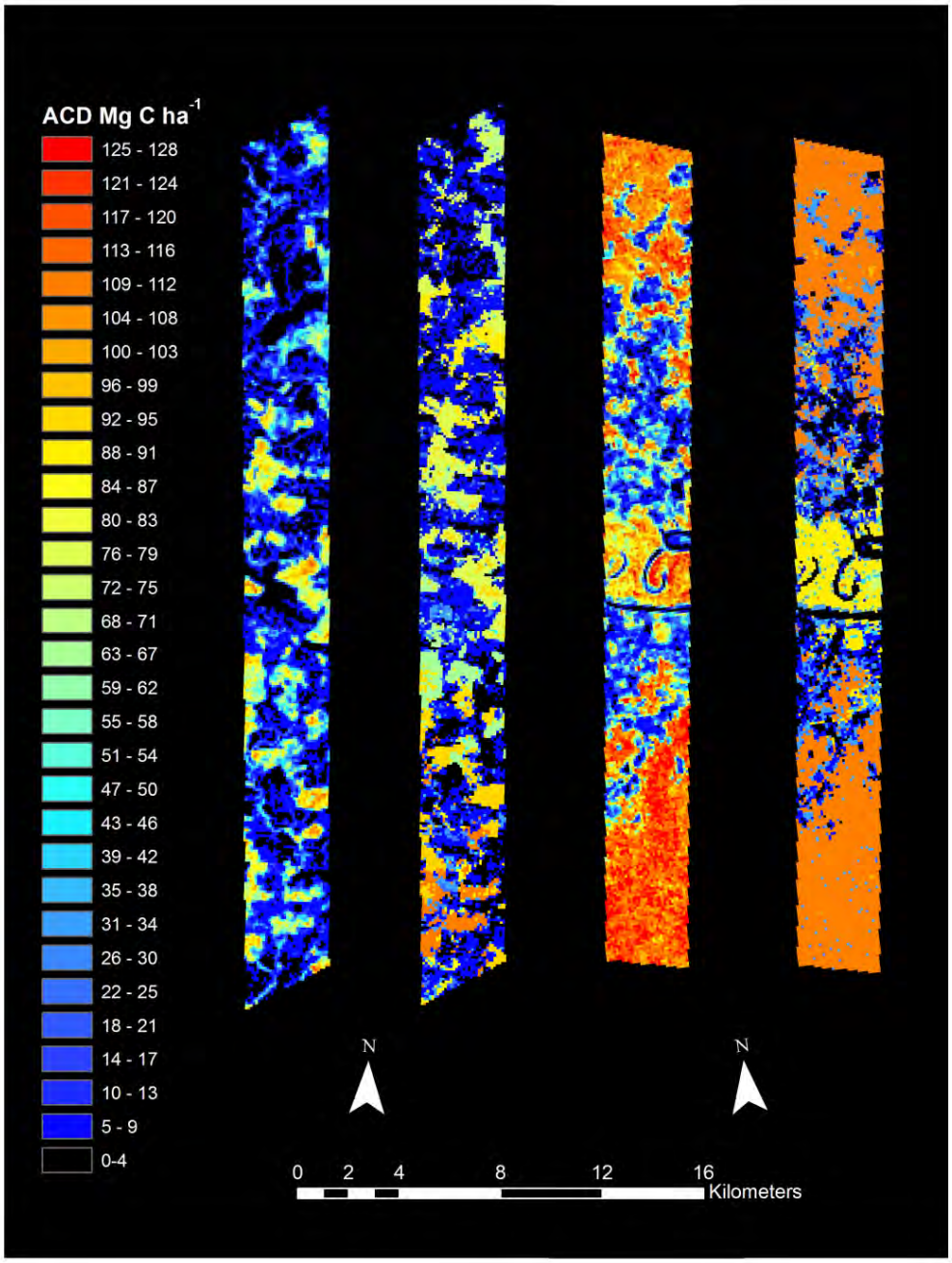

Figure S5. Side-by-side comparison of LiDAR-based ACD (left) and regionally-mapped ACD (right) according to the stratification approach.

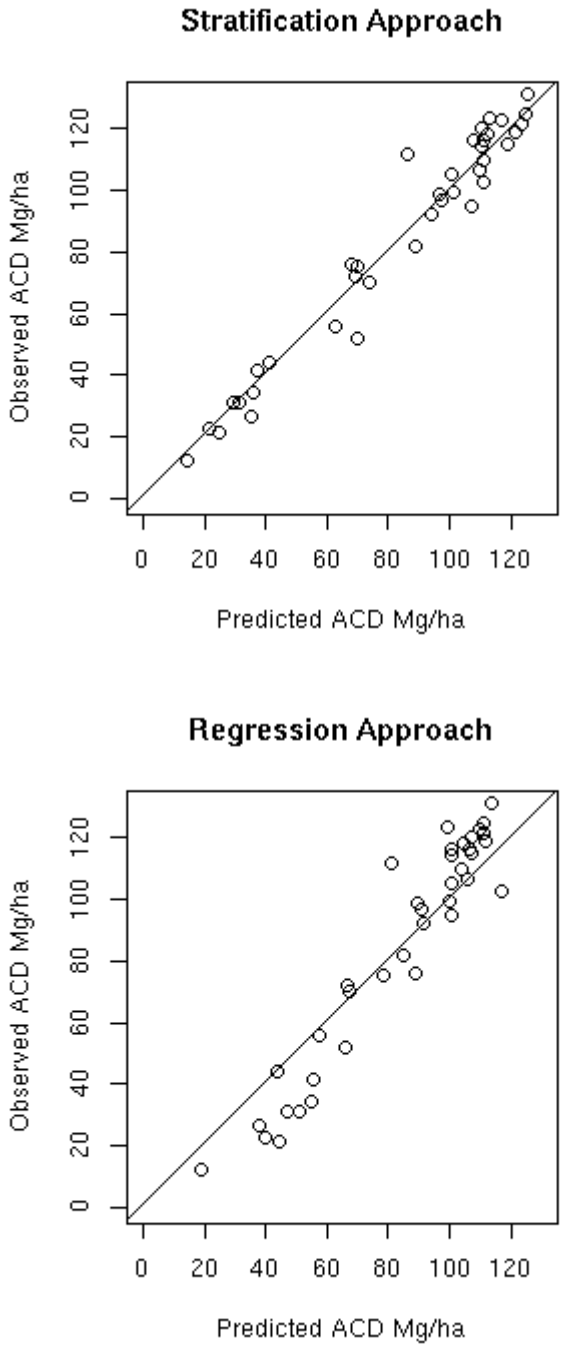

Figure S6. Mean aboveground carbon density (ACD; Mg/ha) as predicted by the stratification and regression approaches to upscaling, compared to the observed estimate derived from airborne LiDAR. Each point represents the validation region of one of 38 flight polygons. These areas comprise the 25% of the LiDAR coverage remaining after excluding a 2600 m strip down the center of each polygon that was used to train the upscaling models. The line depicts a 1:1 relationship.

Table S1. Allometric models used to estimate aboveground biomass (AGB; kg) or height (H; m). Diameters (D, cm) were measured at breast height (1.3 m from the base) or above buttress. Wood densities (ρ; g cm^{-3}) were taken from a global wood density database (Chave et al., 2009) based on species-, genus-, or family-level identification (see Table S2).

Parameter	Equation	r^2	Reference
AGB	$0.0776*(D^2*H*\rho)^{0.94}$	0.96[1]	Chave et al. (2005)
H	$5.2497*D^{0.4258}$	0.68	This study
AGB	$\pi*(0.5*D)^2*\rho*H/10$	n/a[2]	Asner et al. (2010)
AGB	$\pi*(0.5*D)^2*(1.17*\rho-0.21)*H/10*0.5$	n/a[2]	Asner et al. (2010)

[1] coefficient of determination for ln(y)

[2] Palm and dead tree biomass was estimated using the formula for volume of a cylinder, corrected for wood density, and in the case of dead trees for trunk taper and decay typical of standing dead Amazonian trees (Chao et al., 2009).

Table S2. Summary of all stems encountered in the field validation plots. Wood densities were taken from Chave et al. (2009) according to either family or genus-level identification. When a value was not available from Chave et al. (2009), a default regional value of 0.58 was applied (ter Steege et al., 2006).

Family	Genus	Species	Number of Stems	Wood Density (g cm^{-3})	WD Determination	Reference
ANACARDIACEAE			2	0.56	Family	Chave
ANACARDIACEAE	*Tapirira*	spp.	6	0.37	Genus	Chave
ANNONACEAE			37	0.56	Family	Chave
ANNONACEAE	*Duguetia*	spp.	1	0.73	Genus	Chave
ANNONACEAE	*Xylopia*	spp.	36	0.59	Genus	Chave
APOCYNACEAE			33	0.57	Family	Chave
APOCYNACEAE	*Aspidosperma*	spp.	15	0.75	Genus	Chave
APOCYNACEAE	*Couma*	*macrocarpa*	1	0.53	Genus	Chave
APOCYNACEAE	*Couma*	spp.	3	0.53	Genus	Chave
APOCYNACEAE	*Hymatanthus*	spp.	1	0.55	Genus	Chave
ARALIACEAE	*Schefflera*	spp.	2	0.39	Genus	Chave
ARECACEAE			1	0.56	Family	Chave
ARECACEAE	*Astrocaryum*	spp.	1	0.51	Genus	Chave
ARECACEAE	*Euterpe*	*precatoria*	9	0.39	Genus	Chave
ARECACEAE	*Iriartea*	spp.	1	0.27	Genus	Chave
ARECACEAE	*Mauritiella*	spp.	8	0.58	Region	Default
ARECACEAE	*Oenocarpus*	*bacaba*	1	0.68	Genus	Chave
ARECACEAE	*Oenocarpus*	*bataua*	45	0.68	Genus	Chave
ARECACEAE	*Oenocarpus*	spp.	10	0.68	Genus	Chave
ARECACEAE	*Socratea*	*exhorriza*	2	0.23	Genus	Chave
BIGNONIACEAE	*Callychlamys*	spp.	1	0.58	Region	Default
BIXACEAE	*Bixa*	spp.	2	0.35	Genus	Chave
BOMBACACEAE			9	0.48	Family	Chave
BOMBACACEAE	*Pachira*	spp.	2	0.48	Genus	Chave
BOMBACACEAE	*Scleronema*	spp.	9	0.61	Genus	Chave
BURSERACEAE			21	0.52	Family	Chave
BURSERACEAE	*Dacryodes*	spp.	1	0.57	Genus	Chave
BURSERACEAE	*Protium*	spp.	8	0.57	Genus	Chave
CAESALPINIACEAE			36	0.68	Family	Chave
CAESALPINIACEAE	*Hymenaea*	spp.	1	0.80	Genus	Chave
CAESALPINIACEAE	*Macrolobium*	spp.	19	0.62	Genus	Chave
CAESALPINIACEAE	*Tachigali*	spp.	16	0.58	Genus	Chave
CARYOCARIACEAE			1	0.70	Family	Chave
CARYOCARIACEAE	*Caryocar*	spp.	4	0.69	Genus	Chave
CECROPIACEAE			4	0.34	Family	Chave

Family	Genus	Species	Number of Stems	Wood Density (g cm^{-3})	WD Determination	Reference
CECROPIACEAE	*Cecropia*	spp.	2	0.34	Genus	Chave
CECROPIACEAE	*Pourouma*	spp.	13	0.39	Genus	Chave
CELASTRACEAE			5	0.66	Family	Chave
CELASTRACEAE	*Goupia*	*glabra*	2	0.73	Genus	Chave
CELASTRACEAE	*Goupia*	spp.	1	0.73	Genus	Chave
CELASTRACEAE	*Lagupia*	spp.	1	0.58	Region	Default
CHRYSOBALANACEAE			67	0.78	Family	Chave
CHRYSOBALANACEAE	*Licania*	spp.	4	0.82	Genus	Chave
CLUSIACEAE			8	0.65	Family	Chave
CLUSIACEAE	*Caraipa*	spp.	4	0.66	Genus	Chave
CLUSIACEAE	*Clusia*	spp.	3	0.68	Genus	Chave
CLUSIACEAE	*Tovomita*	spp.	7	0.70	Genus	Chave
CLUSIACEAE	*Vismia*	spp.	3	0.49	Genus	Chave
COMBRETACEAE			1	0.60	Family	Chave
COMBRETACEAE	*Buchenavia*	spp.	4	0.75	Genus	Chave
COMBRETACEAE	*Conceveiba*	spp.	1	0.41	Genus	Chave
EBENACEAE	*Dyospiros*	spp.	1	0.68	Genus	Chave
ELAEOCARPACEAE			5	0.55	Family	Chave
ELAEOCARPACEAE	*Sloanea*	spp.	3	0.61	Genus	Chave
EUPHORBIACEAE			10	0.51	Family	Chave
EUPHORBIACEAE	*Conceveiba*	spp.	7	0.41	Genus	Chave
EUPHORBIACEAE	*Hevea*	spp.	73	0.48	Genus	Chave
EUPHORBIACEAE	*Mabea*	spp.	14	0.61	Genus	Chave
EUPHORBIACEAE	*Senefeldera*	spp.	9	0.78	Genus	Chave
FABACEAE			45	0.68	Family	Chave
FABACEAE	*Clatrotropis*	*macrocarpa*	1	0.79	Genus	Chave
FABACEAE	*Clatrotropis*	spp.	75	0.79	Genus	Chave
FABACEAE	*Ormosia*	spp.	2	0.58	Genus	Chave
FABACEAE	*Swartzia*	spp.	1	0.85	Genus	Chave
HUMIRIACEAE			8	0.77	Family	Chave
ICACINACEAE			12	0.58	Family	Chave
LAURACEAE			50	0.56	Family	Chave
LAURACEAE	*Ocotea*	spp.	5	0.54	Genus	Chave
LECYTHIDACEAE			113	0.70	Family	Chave
LECYTHIDACEAE	*Eschweilera*	spp.	12	0.83	Genus	Chave
MELASTOMATACEAE			3	0.67	Family	Chave
MELASTOMATACEAE	*Miconia*	spp.	1	0.63	Genus	Chave
MIMOSACEAE			5	0.68	Family	Chave
MIMOSACEAE	*Inga*	spp.	13	0.58	Genus	Chave
MIMOSACEAE	*Parkia*	spp.	17	0.46	Genus	Chave

Family	Genus	Species	Number of Stems	Wood Density (g cm^{-3})	WD Determination	Reference
MIMOSACEAE	*Zygia*	spp.	16	0.82	Genus	Chave
MORACEAE			65	0.54	Family	Chave
MORACEAE	*Ficus*	spp.	1	0.41	Genus	Chave
MORACEAE	*Pseudolmedia*	spp.	2	0.67	Genus	Chave
MYRISTICACEAE			33	0.51	Family	Chave
MYRISTICACEAE	*Iryanthera*	spp.	30	0.59	Genus	Chave
MYRISTICACEAE	*Virola*	spp.	34	0.48	Genus	Chave
MYRTACEAE			33	0.77	Family	Chave
NYCTAGINACEAE			2	0.52	Family	Chave
OLACACEAE			3	0.76	Family	Chave
OLACACEAE	*Minquartia*	spp.	4	0.79	Genus	Chave
POLYGONACEAE	*Coccoloba*	spp.	2	0.69	Genus	Chave
RUBIACEAE			56	0.64	Family	Chave
SAPINDACEAE			6	0.69	Family	Chave
SAPINDACEAE	*Allophyllus*	spp.	4	0.52	Genus	Chave
SAPINDACEAE	*Cupania*	spp.	2	0.61	Genus	Chave
SAPOTACEAE			151	0.70	Family	Chave
SAPOTACEAE	*Manilkara*	spp.	3	0.89	Genus	Chave
SAPOTACEAE	*Micropholis*	spp.	20	0.66	Genus	Chave
SAPOTACEAE	*Pouteria*	spp.	6	0.69	Genus	Chave
STERCULIACEAE			5	0.48	Family	Chave
STERCULIACEAE	*Sterculia*	spp.	5	0.40	Genus	Chave
STERCULIACEAE	*Theobroma*	spp.	4	0.53	Genus	Chave
TILIACEAE			14	0.48	Family	Chave
TILIACEAE	*Apeiba*	spp.	24	0.25	Genus	Chave
TILIACEAE	*Mollia*	spp.	12	0.49	Genus	Chave
VERBENACEAE	*Vitex*	spp.	1	0.57	Genus	Chave
VIOLACEAE			4	0.65	Family	Chave
VIOLACEAE	*Rinorea*	spp.	1	0.68	Genus	Chave
VOCHYSIACEAE			19	0.55	Family	Chave
VOCHYSIACEAE	*Erisma*	spp.	42	0.57	Genus	Chave
VOCHYSIACEAE	*Qualea*	spp.	3	0.65	Genus	Chave
VOCHYSIACEAE	*Vochysia*	spp.	2	0.49	Genus	Chave
Unknown			499	0.58	Region	Default
Total stems			**2068**			
Unweighted mean WD				**0.59**		
% Family determination					**41.92**	
% Genus determination					**33.46**	
% Region determination					**24.61**	

Table S3. Summary of vegetation classes used in final regional stratification. Elevation (m) a.s.l. (ELEV), fractional cover (%) of photosynthetic vegetation (PV), terrain ruggedness index (TRI), and catchment (CM) are shown. Mean, median, and standard deviation of LiDAR-based aboveground carbon density (ACD) are given in Mg C ha^{-1}. Total extent of LiDAR coverage (ha) and total extent of each class in the regional ACD map (ha) are provided, as well as the relative coverage of LiDAR (%) within each class. An asterisk (*) indicates that ACD statistics were calculated from a broader class due to < 100 ha of LiDAR coverage.

CLASS NUMBER		ELEV	PV	TRI	CM	Mean ACD	Median ACD	St. Dev. ACD	LiDAR (ha)	Map (ha)	Cover (%)
Non-forest											
1			(0,20]			3.1	0.2	8.7	944	42429	2.22
2			(20,40]			4.0	0.4	10.8	6152	226653	2.71
3			(40,60]			4.3	0.6	10.8	22661	735553	3.08
4			(60,80]			12.9	5.4	22.7	35437	1062902	3.33
5			(80,100]			40.5	32.9	35.4	6296	216462	2.91
Deforestation regrowth											
6	5 Years					29.8	21.8	28.9	582	21356	2.73
7	10 Years					30.4	23.1	26.5	2230	57978	3.85
Disturbance regrowth											
8	All ages					53.0	46.6	38.5	1022	31506	3.24
Forest											
9*		< 100	[80,84)			98.6	100.3	26.6	15	4314	0.35
10		< 100	≥ 97			98.4	100.7	28.5	105	5339	1.96
11		[100,125)	[80,84)			74.0	73.3	37.5	113	4254	2.67
12		[100,125)	≥ 97			67.2	67.3	34.1	178	4896	3.64
13		[125,150)	[80,84)			85.7	86.2	36.1	914	9442	9.68
14		[125,150)	≥ 97			107.7	111.5	38.6	277	4864	5.69
15		[150,175)	[80,84)			87.0	91.1	43.9	487	11998	4.06
16		[150,175)	≥ 97			108.4	107.0	39.3	142	4291	3.31
17		[175,200)	[80,84)			48.8	39.6	39.0	1100	22577	4.87
18		[175,200)	≥ 97			90.7	88.1	42.7	664	17021	3.90
19		[200,225)	[80,84)			37.0	25.0	35.0	1683	43820	3.84
20*		[200,225)	≥ 97			104.7	105.1	49.3	671	36875	1.82
21		[225,250)	[80,84)			41.4	32.6	35.4	1518	44846	3.38
22		[225,250)	≥ 97			90.2	86.7	30.9	1322	62927	2.10
23		[250,275)	[80,84)			41.7	31.9	35.6	849	40519	2.10
24		[250,275)	≥ 97			92.0	89.8	29.4	651	56393	1.15
25		[275,300)	[80,84)			41.1	29.9	35.8	587	25592	2.29
26		[275,300)	≥ 97			88.2	86.8	22.5	1499	31768	4.72
27		[300,325)	[80,84)			33.1	20.0	36.5	415	14345	2.90
28		[300,325)	≥ 97			89.0	86.9	25.9	1384	27924	4.96

29	[325,350)	[80,84)			25.8	15.1	30.7	418	9174	4.55
30	[325,350)	≥ 97			91.9	92.6	35.2	535	24660	2.17
31	[350,375)	[80,84)			31.3	19.8	32.3	268	6112	4.39
32	[350,375)	≥ 97			82.7	81.9	37.9	349	19915	1.75
33	[375,400)	[80,84)			36.6	24.2	34.4	244	4576	5.33
34	[375,400)	≥ 97			81.9	83.3	29.3	464	13962	3.32
35	[400,500)	[80,84)			35.7	17.9	39.1	673	9498	7.09
36	[400,500)	≥ 97			69.4	65.7	31.3	664	27491	2.42
37	≥ 500	[80,84)			33.1	16.4	35.0	600	8175	7.34
38	≥ 500	≥ 97			72.4	74.6	34.5	142	15284	0.93
39	< 100	[84,97)	[0,5)		92.5	89.2	30.6	451	17746	2.54
40*	< 100	[84,97)	≥ 5	F	98.8	100.4	26.3	0	53342	0.00
41	< 100	[84,97)	≥ 5	H	98.8	100.4	26.3	2129	99273	2.14
42	[100, 125)	[84,97)	[0,5)		40.3	19.9	39.9	738	27057	2.73
43	[100, 125)	[84,97)	≥ 5	F	118.7	119.9	25.9	1051	295063	0.36
44	[100, 125)	[84,97)	≥ 5	H	112.7	118.4	39.3	8159	480575	1.70
45	[125, 150)	[84,97)	[0,5)		89.5	96.1	33.9	2521	22465	11.22
46	[125, 150)	[84,97)	≥ 5	F	134.7	137.4	30.7	12033	487044	2.47
47	[125, 150)	[84,97)	≥ 5	H	125.3	126.6	28.7	35978	894347	4.02
48*	[125, 150)	[84,97)	≥ 5	I	127.7	129.0	29.5	0	1075	0.00
49	[150, 175)	[84,97)	[0,5)		89.1	92.6	25.5	3120	64763	4.82
50*	[150, 175)	[84,97)	≥ 5	C	124.4	124.5	29.2	0	288	0.00
51	[150, 175)	[84,97)	≥ 5	D	67.5	70.0	19.7	308	854	35.99
52	[150, 175)	[84,97)	≥ 5	F	118.7	118.1	34.1	8334	498378	1.67
53*	[150, 175)	[84,97)	≥ 5	G	124.4	124.5	29.2	0	59239	0.00
54	[150, 175)	[84,97)	≥ 5	H	127.3	126.5	26.0	22558	570354	3.96
55*	[150, 175)	[84,97)	≥ 5	I	124.4	124.5	29.2	0	3685	0.00
56	[175, 200)	[84,97)	[0,5)		70.4	72.5	32.0	1519	28143	5.40
57	[175, 200)	[84,97)	≥ 5	C	54.8	55.1	26.9	6022	51134	11.78
58	[175, 200)	[84,97)	≥ 5	D	84.8	84.7	26.7	6124	64085	9.56
59	[175, 200)	[84,97)	≥ 5	F	111.8	112.9	29.6	20528	789486	2.60
60	[175, 200)	[84,97)	≥ 5	G	85.2	87.6	33.9	1151	333779	0.34
61	[175, 200)	[84,97)	≥ 5	H	119.5	120.3	25.3	15989	762784	2.10
62*	[175, 200)	[84,97)	≥ 5	I	103.4	107.4	34.9	0	2491	0.00
63	[200, 225)	[84,97)	[0,5)		47.9	46.5	35.9	2085	108875	1.91
64	[200, 225)	[84,97)	≥ 5	C	46.5	44.5	28.5	4262	120186	3.55
65	[200, 225)	[84,97)	≥ 5	D	71.6	70.2	30.3	4185	201630	2.08
66	[200, 225)	[84,97)	≥ 5	E	73.0	71.9	28.1	1920	42735	4.49
67	[200, 225)	[84,97)	≥ 5	F	114.7	116.4	29.5	23211	759033	3.06
68	[200, 225)	[84,97)	≥ 5	G	102.8	107.2	29.7	3240	395970	0.82
69	[200, 225)	[84,97)	≥ 5	H	114.2	116.6	25.6	18553	794812	2.33
70*	[200, 225)	[84,97)	≥ 5	I	103.9	109.6	35.3	0	898	0.00
71	[225, 250)	[84,97)	[0,5)		73.1	70.4	36.2	747	30607	2.44

72	[225, 250)	[84,97)	≥ 5	C	54.5	54.8	23.6	6861	293979	2.33
73	[225, 250)	[84,97)	≥ 5	D	56.7	55.5	28.7	1159	101518	1.14
74	[225, 250)	[84,97)	≥ 5	E	106.4	107.7	25.7	15949	261248	6.10
75	[225, 250)	[84,97)	≥ 5	F	110.3	113.0	28.0	20096	667876	3.01
76	[225, 250)	[84,97)	≥ 5	G	105.2	109.6	31.4	2400	204874	1.17
77	[225, 250)	[84,97)	≥ 5	H	109.6	112.7	27.8	21715	921188	2.36
78*	[225, 250)	[84,97)	≥ 5	I	102.5	107.4	32.3	0	<1	0.00
79	[250, 275)	[84,97)	[0,5)		80.6	82.3	25.5	1807	61716	2.93
80	[250, 275)	[84,97)	≥ 5	C	63.2	63.6	25.2	5899	288751	2.04
81	[250, 275)	[84,97)	≥ 5	D	75.1	75.1	49.8	173	22553	0.77
82	[250, 275)	[84,97)	≥ 5	E	102.2	102.1	23.4	2978	129279	2.30
83	[250, 275)	[84,97)	≥ 5	F	98.8	99.5	27.0	13517	475777	2.84
84*	[250, 275)	[84,97)	≥ 5	G	92.6	94.9	31.8	29	114640	0.02
85	[250, 275)	[84,97)	≥ 5	H	101.7	106.7	33.0	6906	338265	2.04
86	[275, 300)	[84,97)	[0,5)		79.3	79.1	17.5	699	6985	10.01
87	[275, 300)	[84,97)	≥ 5	C	74.7	76.6	24.4	5307	147247	3.60
88*	[275, 300)	[84,97)	≥ 5	D	86.3	88.1	28.0	62	6110	1.02
89	[275, 300)	[84,97)	≥ 5	E	100.4	98.9	19.4	1083	17128	6.32
90	[275, 300)	[84,97)	≥ 5	F	90.1	91.8	26.4	12727	340886	3.73
91*	[275, 300)	[84,97)	≥ 5	G	86.3	88.1	28.0	0	42191	0.00
92	[275, 300)	[84,97)	≥ 5	H	85.8	91.3	39.5	1650	69960	2.36
93*	[300, 325)	[84,97)	[0,5)		86.1	90.2	34.3	82	2228	3.68
94	[300, 325)	[84,97)	≥ 5	C	77.9	79.1	25.7	2389	87873	2.72
95	[300, 325)	[84,97)	≥ 5	D	66.8	40.7	74.2	102	2073	4.92
96	[300, 325)	[84,97)	≥ 5	E	104.3	104.2	19.5	2678	21621	12.39
97	[300, 325)	[84,97)	≥ 5	F	84.6	89.6	37.6	5607	123349	4.55
98*	[300, 325)	[84,97)	≥ 5	G	86.1	90.2	34.3	0	11702	0.00
99	[300, 325)	[84,97)	≥ 5	H	66.4	65.8	36.3	931	26436	3.52
100*	[325, 350)	[84,97)	[0,5)		76.0	77.9	40.6	28	825	3.42
101	[325, 350)	[84,97)	≥ 5	C	58.6	56.0	37.2	534	56166	0.95
102	[325, 350)	[84,97)	≥ 5	D	50.4	38.7	50.5	135	909	14.85
103	[325, 350)	[84,97)	≥ 5	E	100.7	100.9	18.6	749	14654	5.11
104	[325, 350)	[84,97)	≥ 5	F	75.7	75.3	41.3	3886	39293	9.89
105*	[325, 350)	[84,97)	≥ 5	G	76.1	78.0	40.6	0	6128	0.00
106	[325, 350)	[84,97)	≥ 5	H	69.3	63.5	41.4	582	17649	3.30
107*	[350, 375)	[84,97)	[0,5)		68.7	65.5	36.4	43	294	14.62
108	[350, 375)	[84,97)	≥ 5	C	66.2	67.0	30.4	1500	40794	3.68
109	[350, 375)	[84,97)	≥ 5	D	48.2	41.4	32.9	184	733	25.12
110*	[350, 375)	[84,97)	≥ 5	E	68.9	65.8	36.4	0	6451	0.00
111	[350, 375)	[84,97)	≥ 5	F	72.9	68.1	39.6	1902	19698	9.65
112*	[350, 375)	[84,97)	≥ 5	G	68.9	65.8	36.4	0	3259	0.00
113	[350, 375)	[84,97)	≥ 5	H	69.3	65.1	38.4	555	16925	3.28
114*	[375, 400)	[84,97)	[0,5)		71.9	70.0	35.6	7	179	4.01

115	[375, 400)	[84,97)	≥ 5	C	66.1	66.7	29.7	1988	28200	7.05
116	[375, 400)	[84,97)	≥ 5	D	47.9	45.8	22.5	165	617	26.74
117*	[375, 400)	[84,97)	≥ 5	E	71.9	69.9	35.6	0	96	0.00
118	[375, 400)	[84,97)	≥ 5	F	81.4	80.3	39.4	1018	11487	8.86
119*	[375, 400)	[84,97)	≥ 5	G	71.9	69.9	35.6	0	1420	0.00
120	[375, 400)	[84,97)	≥ 5	H	80.6	79.6	41.6	661	17462	3.79
121*	[400, 500)	[84,97)	[0,5)		70.5	66.9	38.3	2	1726	0.14
122	[400, 500)	[84,97)	≥ 5	C	61.3	60.4	29.6	1779	73418	2.42
123	[400, 500)	[84,97)	≥ 5	D	50.6	50.6	21.8	598	1350	44.25
124*	[400, 500)	[84,97)	≥ 5	E	70.5	66.9	38.3	0	40	0.00
125	[400, 500)	[84,97)	≥ 5	F	73.0	71.5	39.5	3691	23530	15.69
126*	[400, 500)	[84,97)	≥ 5	G	70.5	66.9	38.3	0	4129	0.00
127	[400, 500)	[84,97)	≥ 5	H	79.1	82.0	42.5	2225	33796	6.58
128*	≥ 500	[84,97)	[0,5)		57.2	49.4	37.0	1	107	1.34
129*	≥ 500	[84,97)	≥ 5	A	57.2	49.4	37.0	0	<1	0.00
130*	≥ 500	[84,97)	≥ 5	B	57.2	49.4	37.0	0	<1	0.00
131*	≥ 500	[84,97)	≥ 5	C	57.2	49.4	37.0	0	56747	0.00
132*	≥ 500	[84,97)	≥ 5	D	57.2	49.4	37.0	0	9	0.00
133*	≥ 500	[84,97)	≥ 5	E	57.2	49.4	37.0	0	48	0.00
134	≥ 500	[84,97)	≥ 5	F	45.0	33.8	34.5	1827	26001	7.03
135*	≥ 500	[84,97)	≥ 5	G	57.2	49.4	37.0	0	6834	0.00
136	≥ 500	[84,97)	≥ 5	H	70.0	74.1	35.2	1745	7913	22.06